

5400

69-40  
DND

PREPRINT

---

IN-SITU STRESS DETERMINATION AT GREAT DEPTH BY MEANS  
OF HYDRAULIC FRACTURING

By

B. Haimson and C. Fairhurst

To be Presented at the Eleventh Symposium on Rock Mechanics  
June 16-19, 1969  
Berkeley

**LIBRARY COPY**  
Materials & Research Dept.

PREPRINT

IN-SITU STRESS DETERMINATION AT GREAT DEPTH BY MEANS  
OF HYDRAULIC FRACTURING

By

B. Haimson and C. Fairhurst

To be Presented at the Eleventh Symposium on Rock Mechanics  
June 16-19, 1969  
Berkeley

IN-SITU STRESS DETERMINATION AT GREAT DEPTH BY MEANS OF  
HYDRAULIC FRACTURING

by

BEZALEL HAIMSON\* AND CHARLES FAIRHURST  
UNIVERSITY OF MINNESOTA,  
MINNEAPOLIS, MINNESOTA

ABSTRACT

This paper summarizes a theoretical and experimental investigation of the method of hydraulic fracturing as a technique of stress measurement in brittle, elastic, isotropic, porous and non-porous formations. Theoretically, a general relationship between fracture initiation pressure and tectonic principal stresses is found by incorporating the additional stress field created in the case of fracturing fluid penetration into the surrounding rock. It is asserted that if the axis of the vertical borehole is parallel to one of the principal in-situ stresses, and if Kehle's model correctly represents the function of the packers, hydraulic fractures will initiate either vertically or horizontally depending on the stress distribution at the borehole.

Laboratory tests on simulated boreholes show that the critical internal pressures necessary to induce fractures were a function of the simulated in-situ stresses, as anticipated by the theoretical criteria for fracture initiation. All fractures were tensile ruptures, oriented in either the vertical or the horizontal plane,

---

\* Presently with Halliburton Services, Duncan, Oklahoma.

depending on the external loading conditions and on the type of packers used. When rubber packers were employed only vertical fractures were obtained. This result is significant in that additional information on the horizontal principal in-situ stresses can thus be gained in some cases. All vertical fractures were perpendicular to the smaller horizontal compressive load. The effect of hole size and pressurizing rate on hydraulic fracturing pressures was also determined.

In addition to the reported experimental results, recently published oil field tests also indicate a strong relationship between tectonic stresses and hydraulic fracturing. In conclusion, the method appears capable of providing good approximations of in-situ stresses at great depth.

depending on the external loading conditions and on the type of packers used. When rubber packers were employed only vertical fractures were obtained. This result is significant in that additional information on the horizontal principal in-situ stresses can thus be gained in some cases. All vertical fractures were perpendicular to the smaller horizontal compressive load. The effect of hole size and pressurizing rate on hydraulic fracturing pressures was also determined.

In addition to the reported experimental results, recently published oil field tests also indicate a strong relationship between tectonic stresses and hydraulic fracturing. In conclusion, the method appears capable of providing good approximations of in-situ stresses at great depth.

## INTRODUCTION

One of the main functions of rock mechanics research has been to find ways of determining in-situ stresses. Many methods have been suggested, the most significant ones calling for measurements inside boreholes. These methods usually employ some instrumentation for the purpose of measuring hole deformation. Several years ago, a new method was suggested by Scheidegger<sup>1</sup>, based on previous work by Hubbert and Willis<sup>2</sup>. It was the method of "hydraulic fracturing", which had been introduced by the oil industry in 1948 for the purpose of oil well production stimulation. Basically, hydraulic fracturing consists of sealing off a section of a borehole, pumping in a fluid, and pressurizing it until fracture occurs. If pumping is continued vigorously, the fracture is opened up and extended. In an oil field, such an artificial fracture increases the overall permeability of the formation and usually enhances production. During the entire operation, the variation of pressure with time is ordinarily recorded.

Hubbert<sup>2</sup>, Scheidegger<sup>1</sup>, Kehle<sup>3</sup> and others have shown that the recorded pressures can be theoretically related to the magnitudes of the principal in-situ stresses; the orientation of the fracture can often be used to determine the direction of the principal stresses. The advantage of hydraulic fracturing over the present in-situ stress determination methods is simplicity: no sophisticated instrumentation is required inside the borehole; hence, the stresses can be measured at any depth. Moreover, if the formation is impermeable to the fracturing fluid, no elastic constants of the rock

are required in calculating the stresses, a factor that not only simplifies the problem, but renders the results more reliable.

It was felt, however, that as most rocks are porous-permeable, the influence of stresses due to fluid flow into the formation should also be considered in determining the in-situ stress distribution. Furthermore, although there exists quite an extensive literature on the theoretical basis of hydraulic fracturing, very little had been done to verify the results experimentally. The present paper, based mainly on the Ph. D. thesis undertaken by one of the authors<sup>4</sup>, attempts to extend the criterion for hydraulic fracturing and to report on some laboratory tests on simulated boreholes. Some interesting field results are also mentioned.

## THEORETICAL CONSIDERATIONS

In order to establish the stress distribution in a formation and relate it to hydraulic fracturing pressures, some assumptions are made regarding the materials involved. The rock is brittle elastic, homogeneous, isotropic, linear and porous. The injected fluid flows through the pores according to Darcy's Law. Following Biot<sup>5</sup>, a complete analogy exists between the elasticity of a porous material, like the one described above, and thermoelasticity. Hence, solutions to problems in thermoelasticity may be used to obtain solutions to problems of porous materials.

Prior to drilling of the borehole, the state of stress at a point, situated at a depth  $D$  from the surface, is generally non-hydrostatic. To simplify the problem, it is assumed that one of the principal tectonic stresses ( $S_{33}$ ) acts in the vertical direction. This is justified in most formations (see Anderson<sup>6</sup>). Taking tensile stresses as positive, the larger horizontal tectonic stress is  $S_{22}$  and the smaller is  $S_{11}$ .

When a vertical circular borehole is introduced, the tectonic stresses redistribute themselves around the cylindrical cavity according to Kirsch's solution<sup>7</sup>. With the pressurization of the borehole at the required depth, two additional stress fields arise. One is due to the pressure  $P_w$  at the borehole wall which can be viewed as an internal pressure acting on a hollow infinitely thick cylinder. The other stress field is introduced if the fracturing fluid used to pressurize the borehole actually penetrates the formation and flows through its pores. Its stress distribution can be



determined by using Nowacki's<sup>8</sup> solution to thermal inclusions in hollow infinite cylinders and utilizing the analogy between thermo-elasticity and porous-elasticity.<sup>4</sup>

The complete stress distribution around the borehole is obtained by superposing the three stress fields mentioned above. At the borehole wall and away from the ends of the pressurized interval, the complete principal stresses are:

$$S_{rr} = -P_w$$

$$S_{\theta\theta} = S_{11} + S_{22} - 2(S_{11} - S_{22}) \cos 2\theta + P_w - \alpha \frac{1 - 2\nu}{1 - \nu} (P_w - P_o)$$

$$S_{zz} = S_{33} - 2\nu(S_{11} - S_{22}) \cos 2\theta - \alpha \frac{1 - 2\nu}{1 - \nu} (P_w - P_o) \dots \dots \dots (1)$$

where:

$P_o$  is the initial pore fluid pressure in the formation.

$\theta$  is the angle measured counterclockwise from the radius in the direction of  $S_{11}$ .

$\nu$  is Poisson's ratio of the rock.

$\alpha$  is the porous-elastic parameter of the rock as defined by Biot.<sup>9</sup> Its value is given by

$$\alpha = 1 - \frac{C_r}{C_b} \text{ and can be found in the laboratory.}^{10}$$

( $C_r$  = material matrix compressibility,  $C_b$  = material bulk compressibility).

Terzaghi<sup>11</sup> and Hubbert<sup>12</sup> have found that failure of porous permeable rock is directly related to the distribution of "effective stresses" ( $\sigma_{ij}$ ), where  $\sigma_{ij} = \begin{matrix} S_{ij} + P & \text{for } i = j \\ S_{ij} & \text{for } i \neq j \end{matrix}$  ( $P$  is the pore fluid pressure). At the borehole wall, the pore pressure in permeable rock is  $P_w$ , while at a great distance from the borehole

the pore pressure remains  $P_0$ . Hence, in terms of effective stresses, equation (1) becomes:

$$\begin{aligned}\sigma_{rr} - P_w &= -P_w \\ \sigma_{\theta\theta} - P_w &= \sigma_{11} + \sigma_{22} - 2P_0 - 2(\sigma_{11} - \sigma_{22}) \cos 2\theta + P_w \\ &\quad - \alpha \frac{1-2\nu}{1-\nu} (P_w - P_0) \\ \sigma_{zz} - P_w &= \sigma_{33} - P_0 - 2\nu(\sigma_{11} - \sigma_{22}) \cos 2\theta - \alpha \frac{1-2\nu}{1-\nu} (P_w - P_0) \\ &\quad \dots\dots\dots(2)\end{aligned}$$

As  $P_w$  is gradually increased, both the tangential and the vertical effective stresses at the borehole can eventually become tensile. The points around the hole where the tangential effective stress is maximum are at  $\theta = 0, \pi$ . There,  $\sigma_{\theta\theta}$  is given by:

$$\sigma_{\theta\theta} = 3\sigma_{22} - \sigma_{11} + (2 - \alpha \frac{1-2\nu}{1-\nu})(P_w - P_0) \dots\dots\dots(3)$$

A vertical tensile fracture at  $\theta = 0, \pi$  will occur when  $P_w$  reaches such a critical value ( $P_c^p$ ), that the effective tangential stress (equation 3) becomes equal or larger than the tensile strength of the rock in the horizontal plane ( $\sigma_t$ ):

$$P_c^p - P_0 = \frac{\sigma_t - 3\sigma_{22} + \sigma_{11}}{2 - \alpha \frac{1-2\nu}{1-\nu}} \dots\dots\dots(4)$$

where  $P_c^p$  is the breakdown (critical) pressure in permeable rock.

As  $0 \leq \alpha \leq 1$  and  $0 \leq \nu \leq 0.5$  for rock, it follows that:

$$1 \leq 2 - \alpha \frac{1-2\nu}{1-\nu} \leq 2 \dots\dots\dots(5)$$

If the rock parameters ( $\sigma_t$ ,  $\nu$ ,  $\alpha$ ) are known, equation (4) gives a direct relationship between the horizontal effective principal stresses and the recorded critical pressure. For rough approximations, it may be assumed that  $\sigma_{11} \approx \sigma_{22}$  ( $= \sigma_H$ ). In this case:

$$P_c^p - P_o = \frac{\sigma_t - 2\sigma_H}{2 - \alpha \frac{1 - 2\nu}{1 - \nu}} \dots\dots\dots(6)$$

where the only unknown is  $\sigma_H$ , the hydrostatic horizontal effective stress.

In rock that is impermeable to the fracturing fluid, the pore pressure is  $P_o$  everywhere, and equations (4) and (6) become:<sup>4</sup>

$$P_c^1 - P_o = \sigma_t - 3\sigma_{22} + \sigma_{11} \dots\dots\dots(7a)$$

$$P_c^1 - P_o = \sigma_t - 2\sigma_H \dots\dots\dots(7b)$$

where  $P_c^1$  is the breakdown (critical) pressure in the impermeable case. Equations (7) are identical to the vertical fracturing criteria suggested by Scheidegger<sup>1</sup>. Knowledge of only one rock parameter is required in this case.  $\sigma_t$  should be measured in the laboratory on identical rock under conditions of simulated hydraulic fracturing in impervious formations. From equations (7),  $\sigma_t$  is then equal to  $P_c^1$  if

$$\sigma_{11} = \sigma_{22} = P_o = 0.$$

From equations (2), a criterion for horizontal fracturing away from the ends of the hole, can also be established:<sup>4</sup>

$$P_c^p - P_o = \frac{\sigma_t^v - \sigma_{33}}{1 - \alpha \frac{1 - 2\nu}{1 - \nu}} \dots\dots\dots(8)$$

where  $\sigma_t^v$  is the tensile strength of the rock in the vertical direction.

If the rock is impermeable to the fracturing fluid,  $P_o$  is the pore pressure everywhere and  $P_w$  does not influence the value of  $\sigma_{zz}$ ; hence, no horizontal fracture initiation is possible in this case. However, horizontal fractures could be started if the borehole wall were precracked or prenotched.

Comparing equations (6) and (8), it is apparent that a horizontal fracture in porous rock would be initiated if the average horizontal tectonic effective stress ( $\sigma_H$ ) were much larger than  $\sigma_{33}$ . This is seldom the case in most formations.

Kehle<sup>3</sup> has investigated the conditions of horizontal fracture initiation near the ends of the pressurized hole. His model included a finite pressurized interval terminated by two solid packers, which under the pressure  $P_w$ , transmitted a shear load to the borehole wall. By incorporating in Kehle's solution, an approximation of the stresses due to injected fluid flow into the formations, the criterion for horizontal fracturing, near one of the hole ends, becomes:<sup>4</sup>

$$P_c^p - P_o \cong \frac{\sigma_t^v - \sigma_{33}}{1.94 - \alpha \frac{1 - 2\nu}{1 - \nu}} \dots\dots\dots(9)$$

In the impermeable case, equation (9) reduces to Kehle's<sup>3</sup> criterion:

$$P_c^i - P_o = \frac{\sigma_t^v - \sigma_{33}}{0.94} \dots\dots\dots(10)$$

In all the above fracturing criteria, the breakdown (critical) pressure in the permeable case ( $P_c^p$ ) is always lower than  $P_c^i$  for an otherwise identical formation under identical tectonic conditions.

It should be noted that Kehle's model has some grave limitations. It assumes that a packer is a rigid cylinder, in full contact with the borehole wall, which, in response to an axial load at one end, applies a shear stress to the rock. In many field applications, however, rubber packers are used. Rubber is a "liquid-solid" elastomer which under the axial load mentioned, would probably apply a similar radial load to the rock. This would have a negative effect on the stress concentration in the vertical direction, and chances of horizontal fracturing would thus be minimized. Experimental results described below seem to verify this hypothesis.

Once the fracture is initiated, additional pumping of fracturing fluid (at bottom hole injection pressure  $P_f$ ) will extend the rupture along the path of least resistance, i.e., perpendicular to the direction of largest principal tectonic stress (smallest compressive stress). When pumping is stopped, with the borehole still sealed, the bottom-hole pressure will be indicative of the pressure in the fracture, for no friction losses will exist (Fig. 1). This "instantaneous shut-in pressure" ( $P_s$ ) is at least equal to the compressive stress that is perpendicular to the fracture plane. If  $P_s$  were smaller than the compressive stress, the fracture would have been closed; if  $P_s$  were much larger than the compressive stress, the fracture would extend an additional amount until a balance was reached. In general, then:

$$P_f \geq P_s \geq -S_{22} \quad (\text{vertical fractures}) \dots \dots \dots (11a)$$

$$P_f \geq P_s \geq -S_{33} \quad (\text{horizontal fractures}) \dots \dots \dots (11b)$$

A number of attempts have been made to establish accurate relationships between  $P_s$  or  $P_f$  and  $S_{22}$  or  $S_{33}$  in both porous and nonporous rock.<sup>13,14,15</sup> All these relationships require knowledge of fracture dimensions which are not measurable as yet. When approximate values are used for width and length of the fracture,  $P_f$  is usually within 300 psi larger than the smallest compressive stress;  $P_s$  is ordinarily within 200 psi. Since the determination of in-situ stresses at great depth is not expected to be very accurate, it can be approximated that  $P_s$  is roughly equal to the smallest compressive stress. If the value of  $P_s$  is not available,  $P_f$  can be used as a rougher estimate.

In summary, the magnitudes of  $P_o$ ,  $P_c$ ,  $P_f$ ,  $P_s$ , which are recorded during a hydraulic fracturing test, provide the basic values from which tectonic stresses can be estimated. The main problem, still to be overcome, is detection of fracture initiation and direction. At the borehole wall, techniques like the borehole televiewer<sup>16</sup> or the oriented impression packer<sup>17</sup> can accurately determine fracture type and azimuth. But no method is yet available that can follow fracture orientation or direction away from the hole. When such a method is found, hydraulic fracturing could be used with confidence at any depth and for any possible stress distribution. However, the situations in which fracture directions away from the hole need to be detected are rare.

When a formation is fractured hydraulically, a number of possibilities exist:

- a. The fracture is vertical. In this case, equations (11a) and (4) or (7a) can be used to uniquely determine  $S_{11}$  and  $S_{22}$ .  $S_{33}$  is generally accepted to be equal to the weight of the overlying rock (sometimes taken as 1 psi/ft. of depth). The directions of  $S_{11}$  and  $S_{22}$  can be found from oriented packer impressions.
- b. The fracture is horizontal. In this case, only  $S_{33}$  can be determined, but it is also noted that  $S_{33}$  is the smallest compressive stress.
- c. The fracture initiates vertically but extends horizontally. This type of fracture can exist when the borehole wall is smooth and not precracked, and the packers used are such that no vertical stress concentration is allowed at the hole ends. Equation (6) or (7b) then provides an estimate of the horizontal principal in-situ stresses, and equation (11b) gives the value of  $S_{33}$  which is also the smallest compressive in-situ stress. Oriented packer impressions will determine the directions of  $S_{11}$  and  $S_{22}$ .  
If the change in inclination from a vertical to a horizontal fracture is achieved gradually, it is theoretically possible that the pressure-versus-time plot would show two levels of  $P_f$  (Fig. 2). The first level ( $P_f^1$ ) would be an approximation of  $-S_{22}$ , and the second level ( $P_f^2$ ) would be approximately equal to  $-S_{33}$ . The decrease from  $P_f^1$  to  $P_f^2$  is understood to occur when the horizontal fracture 'backs up' into the hole. All three principal in-situ stresses can thus be uniquely determined.

d. The fracture initiates horizontally but extends vertically. This case may arise when rigid type packers are used. A vertical stress concentration is then allowed to generate at the hole ends (e.g. Kehle's model) such that the pressure required to induce a horizontal fracture is smaller than the vertical  $P_c$ , although  $-S_{22}$  is the smallest compressive in-situ stress. Equations (9) or (10) will yield  $S_{33}$ , and equation (11a) will give the value of  $S_{22}$ . The direction of  $S_{22}$  cannot normally be determined, since methods of detecting fracture direction away from the borehole have yet to be perfected.

In conclusion, if a section of unprecracked vertical borehole, sealed off by two rubber packers, is hydraulically fractured, possibilities a and c are the most likely to occur, and all three principal tectonic stresses and their orientations can be approximately determined.



## LABORATORY EXPERIMENTS

A laboratory experimental program was undertaken to verify some of the assumptions and results stated in the theoretical section. Simulated boreholes, in rock samples subjected to non-hydrostatic triaxial loading, were hydraulically fractured. The breakdown pressures were recorded and the inclination and direction of fractures were observed. The effect of variables such as the diameter of the hole, rate of pressurizing and type of packers was also determined.

Five rock types were chosen for these experiments. Tennessee Marble and Charcoal Granite were selected for testing the hydraulic fracturing criteria in impermeable rock. Both rocks were finely grained, isotropic and homogeneous. Mankato Dolomite was used for its slight permeability, inhomogeneity and anisotropy. Berea Sandstone and hydrostone (mixture of gypsum cement and water) were chosen for their permeability. The natural rock samples were ordered from quarries. The hydrostone samples were prepared in the laboratory by mixing 30, 32, or 35 parts gypsum cement to 100 parts water (by weight). The process of mixing, molding and curing was identical for all samples.<sup>4</sup> A list of physical properties for each of the rock types is given in Table 1.

Two types of rock samples were used: 'cubical' (5.0 inches x 5.0 inches x 5.5 inches) and cylindrical (5.0 inches in diameter, 6.0 inches high). The flat surfaces of all samples were surface ground for smoothness and parallelism. Simulated vertical boreholes were drilled in the center of all samples. The standard diameter of the holes was 0.30 inch, but in some cases, diameters of 0.45 inch, 0.91 inch, 1.05 inch, 1.20 inch, 1.40 inch were also used. Sometimes, the boreholes were drilled only part way through the samples leaving the rock itself to form the bottom end. In other cases, and especially when rubber packers were used, the holes were drilled all the way through the samples. The rubber packers were made of hard rubber belt-shaped O-rings mounted on a steel shaft through which the injection fluid was pumped into the open hole. In most tests, metal packers were used. They were made of tool steel, 1.75 inch long, and were cemented to the borehole wall with an epoxy adhesive. The upper packer was hollow to allow fluid injection into the packed-off interval. This interval was normally kept at 2.0 inches long.

For the purpose of simulating in-situ stresses, a loading system was designed that applied three mutually perpendicular unequal external loads to the cubical samples. The vertical load was generated by a compression testing machine and was transmitted through an upper steel platen. The latter also served as a channel for the pressurizing fluid flowing toward the simulated borehole.

The lateral loads were applied through four identical flat-jacks that filled the spaces between the sides of the samples and the inner walls of a heavy steel frame (Fig. 3). Each pair of opposite flat-jacks was connected in parallel to a manual hydraulic pump and could be pressurized independently. The loading uniformity was surprisingly good and very satisfactory for the type of tests undertaken.<sup>4</sup> Thus, a truly non-hydrostatic triaxial loading system was achieved.

Cylindrical samples were tested in a standard pressure jacket through which a hydrostatic horizontal loading was applied. Vertical loading was achieved by use of a compression testing machine. This conventional loading system was used for the purpose of comparing results with the flat-jack system whenever the horizontal principal stresses were equal.

The fracturing fluids used were commercial hydraulic oils of different viscosities ranging from 64 to 2100 centipoise. The internal pressurization of all samples was provided by a closed-loop electro hydraulic servo system (Fig. 4). The main advantage of this system was its ability to maintain identical borehole pressurization rates from sample to sample, notwithstanding the amount of fluid leakage into the rock.

The experimental procedure in both cubical and cylindrical samples was essentially the same. First, the predetermined horizontal and vertical external compressive loads were simultaneously

applied. The range of these loads was 0 - 5000 psi. Since the external compressions simulated tectonic stresses, they were kept constant throughout the remainder of the test. The borehole was then pressurized and the pressure-versus-time was recorded in an X-Y plotter by means of a pressure transducer. At some critical pressure ( $P_c$ ), a fracture initiated at the hole boundary. This phenomenon was observed by a sudden drop in the internal pressure and by a sharp increase in the compressive load acting perpendicularly to the plane of the fracture. The experiment was then stopped, and the sample was removed, sectioned and photographed. The sample was thoroughly examined and all pertinent data recorded.

## EXPERIMENTAL RESULTS

This section summarizes the results of some four hundred tests performed on five different rocks. The details of each test can be found in Haimson's thesis<sup>4</sup>. No significant differences were found between the behavior of the cylindrical and the cubical specimens. The results of the Berea Sandstone tests are of a qualitative nature only, since the number of samples available was very limited (fourteen).

### Fracture Type and Inclination

In all of the samples tested, permeable and impermeable, the induced hydraulic fractures were always tensile ruptures. No shear failures were observed.

The inclination of the fractures in all the rock types was either vertical or horizontal (or nearly so) depending on the stress distribution around the simulated borehole.

### Vertical Fractures

All vertical fractures were initiated at the borehole wall and extended in a plane approximately perpendicular to the direction of the smaller horizontal compressive load. Figure 5 shows a horizontal section of a vertically fractured sample of Tennessee Marble. The fracture line is perfectly perpendicular to the smallest compressive load (1300 psi). Another example of a vertical fracture in a brittle, impermeable rock is shown in Figure 6. It is a section of a Charcoal Granite sample exhibiting a fracture normal to the smallest simulated compressive in-situ stress (600 psi). The intersection of a pre-existing crack (shown

between the dashed lines) did not divert the direction of the fracture. A typical vertical fracture in a very permeable rock (Berea Sandstone) is shown in Figure 7. Note that  $\sigma_x$  and  $\sigma_y$  designate horizontal compressive loads;  $\sigma_z$  designates vertical compressive load. The amount of penetration into the sandstone by the injected fluid is clearly visible. The vertical fracture is normal to the smallest compression, just as in the previous samples. Figure 8 shows a hydrostone sample in which the vertical fracture had just reached the outer face when the test was stopped. There was a difference of only 250 psi between  $\sigma_x$  and  $\sigma_y$ , yet the fracture was clearly normal to the smaller  $\sigma_x$ .

Simulated boreholes in which rubber packers were used always yielded vertical fractures, even when the horizontal compressive loads were much larger than the vertical  $\sigma_z$ . In Figure 9 a vertically fractured hydrostone sample is shown. The rubber packer metal shaft and the upper packer are also visible. Two significant things can be observed:  $\sigma_x = \sigma_y = -1800$  psi and  $\sigma_z = -500$  psi; yet the fracture is vertical, and the direction of the fracture is at random. The latter result is due to the hydrostatic horizontal loading, where only a weakness in the rock determined the direction of the rupture. In several cases, including that shown in Figure 10, hydrostatic horizontal loading caused the hydraulic fracture to extend in three different directions, usually at  $120^\circ$  from one another.

In those samples where vertical fractures were initiated, although the compressive  $\sigma_z$  was smaller than either  $\sigma_x$  or  $\sigma_y$ , no change in inclination was observed away from the hole. Theoretically, these fractures were expected to follow the "path of least

resistance" and become gradually horizontal. The discrepancy is attributed to the relatively small size of the rock samples.

In order to compare the experimental values of breakdown (critical) pressure with the anticipated ones (see section on "Theoretical Considerations"), a correction had to be made in Equations (1) to account for the finiteness of the laboratory samples. As this correction was necessary only in the stress field due to fluid flow into the rock, Equations (7) were not affected. In the case of the permeable hydrostone, the corrected Equation (4) became:<sup>4</sup>

$$P_c^P - P_o = \frac{\sigma_t - 3\sigma_{22} + \sigma_{11}}{2 - 0.9\alpha \frac{1 - 2\nu}{1 - \nu}} \dots\dots\dots(12)$$

An identical correction was introduced in Equation (6). Note that in all laboratory experiments there was no initial pore pressure ( $P_o = 0$ ).

Because of the variable nature of the tensile strength, the determination of the value to be used in these tests was made by internally pressurizing samples identical to those used in the bulk of the experiments. No lateral loads were applied, and no injected fluid leak-off was allowed. Thus the value of  $P_c^i$  obtained was equated to  $\sigma_t$ . The average tensile strength values are given in Table 1, as are other rock parameters used (obtained by standard methods).

The comparison between the experimental breakdown pressures and the predicted values from theoretical calculations is presented in this report in the form of graphs based on tables published elsewhere.<sup>4</sup> In the impermeable Charcoal Granite (Fig. 11), the

experimental points are as close as could be expected to the curve based on Equation (7a). In Tennessee Marble, a sudden drop in the experimental points relative to the theoretical curve is observed at about  $P_c = 3000$  psi and above (Fig. 12). This drop may be attributed to minute cracks that have been observed in Tennessee Marble at 3000-4000 psi compression<sup>18</sup>, cracks that undoubtedly lower the tensile strength of the rock. It is rather significant that the experimental results in Mankato Dolomite, the slightly permeable and least homogeneous of the rocks tested, were also close enough to the expected values (Fig. 13). In the case of the permeable hydrostone, the experimental points usually fell somewhere between the  $P_c^1$  and  $P_c^p$  curves (Fig. 14). It was demonstrated, however, that the critical pressures were lower than in the impermeable case and that the  $P_c^p$  line was a close lower limit approximation of the experimental values.

#### Horizontal Fractures

Horizontal fractures were initiated only in those samples where a vertical stress concentration, near the end of the pressurized hole, was possible. When rubber packers were used, no horizontal fractures were obtained even under most favorable conditions (with  $\sigma_z$  being only a fraction of  $\sigma_x$  or  $\sigma_y$ ), suggesting that little vertical stress concentration actually occurred.

However, when steel packers were used, or when the hole was drilled only part way through the sample, horizontal fractures could be obtained. These fractures were always located at the bottom of the hole. Theoretically, both ends give rise to identical



stress concentrations, but the upper packer was hollow to allow the flow of the pressurized fluid toward the open hole. The radial pressure applied by the fluid through the packer and to the rock lowered the stress concentration at the upper end of the hole, thus rendering the bottom of the hole the most vulnerable to horizontal fracturing. Examples of horizontally fractured specimens are shown in Figs. 15, 16 and 17. As noted in the photographs, no difference in type and position of fracture was apparent between the impermeable and the permeable rock.

In comparing the experimental breakdown (critical) pressures to theoretically expected values, it was found that Equations (9) and (10) could be used unchanged, since the correction required to account for the finiteness of the samples was negligible<sup>4</sup>. As to the tensile strength term in Equations (9) and (10), it was found that when  $\sigma_t$  (vertical fractures) was used, the theoretical values of  $P_c$  were invariably lower than the experimental results. However, when only a negligible vertical load was applied, the apparent tensile strength in the vertical direction ( $\sigma_t^V$ ) could be evaluated from Equation (10). The values of  $\sigma_t^V$  can be found in Table 1. One possible reason for the discrepancy between  $\sigma_t$  and  $\sigma_t^V$  is that Kehle's Model did not accurately represent the described laboratory model. With  $\sigma_t^V$  as the tensile strength, the theoretical breakdown pressure curves were a good approximation of the experimental points in the impermeable rock (Fig. 18) and formed the lower limit of test results in the permeable case (Fig. 19).

### Effect of Hole Diameter and Rate of Pressurizing

A series of tests was run on Tennessee Marble and hydrostone samples in which various borehole diameter sizes (0.30 inch-1.40 inch) were used without changing the conditions of external loading and internal pressurization. Figs. 20 and 21 are representative of the results obtained<sup>4</sup>. In the Tennessee Marble samples (Fig. 20), the length of the hole was kept constant (2.0 inches). In hydrostone, both constant hole length and constant length-to-width ratio (Fig. 21) were tried. In all cases, the results show a decrease in breakdown pressure with increase in diameter.

In another series of tests, different pressurizing rates (6, 60, 600 psi/sec) were used on Charcoal Granite and hydrostone. The results show a definite increase in breakdown pressure with increase in pressurizing rate (see for example Figs. 22 and 23).

Clearly, the parameter affected by both diameter change and pressurizing rate is the tensile strength. Hence, in order to determine a realistic value of  $\sigma_t$ , all conditions, including hole size and loading rate, should be kept identical with those of the hydraulic fracturing test itself.

## SUMMARY AND CONCLUSIONS

This paper reports on a theoretical and experimental study of the method of hydraulic fracturing as an instrument of determining regional tectonic stresses at great depth.

Theoretically, the existent criteria for hydraulic fracturing initiation was extended to include the case in which the injected fluid actually penetrates into the porous rock surrounding the borehole. It was found that a main disadvantage exists in the latter case, in that two parameters of the porous-elastic rock ( $\alpha$ ,  $\nu$ ) are needed in relating the breakdown pressure to the principal tectonic stresses. Another significant difference between impermeable and permeable strata is that in the latter, horizontal fracturing away from the hole ends is theoretically possible. However, the tectonic stress distribution required to initiate such a fracture is not very realistic in formations situated at great depth. The applicability of Kehle's Model to the case when rubber packers are used was disputed. It appears that no excessive vertical stress concentration is to be expected at the hole ends, and hence no horizontal fractures near the packers are possible under normal tectonic conditions. Kehle's Model, however, seems to represent boreholes that are sealed off with relatively rigid packers. Using rubber packers, and provided the pressurized borehole is not precracked, the complete tectonic state of stress could be determined in both permeable and impermeable formations, whether or not the smallest compressive tectonic stress acts in the vertical direction.

Laboratory hydraulic fracturing tests on simulated boreholes in both permeable and impermeable rock always resulted in tensile

ruptures. In boreholes sealed with steel packers, the direction of all fractures was either vertical or horizontal (near the bottom of the hole), depending on the loading conditions. When rubber packers were used, only vertical fractures were obtained, regardless of the ratio between the vertical and the horizontal loads. All vertical fractures were perpendicular to the smaller horizontal compressive load. The breakdown (critical) pressures for vertical fractures in the impermeable rock were usually very close to the theoretically anticipated values. In the permeable samples, the theoretical breakdown pressures represented the lower limit of the experimental values. Variations in the rate of pressurizing or in the size of the hole were shown to affect the breakdown pressures, possibly because of changes in the tensile strength parameter. This finding may not be significant in formations at great depth where the tensile strength is considered negligible. But in unprecracked rock, at shallower depths, special care should be paid to the tensile strength values used in estimating tectonic stresses from hydraulic fracturing pressures.

In general, it is felt that this investigation offers a more realistic relationship between hydraulic fracturing pressures and the tectonic stresses, by generalizing the fracturing criteria to include the porous rock case. The experimental results on rubber packers are especially encouraging: by invariably obtaining vertical fractures, the principal tectonic stresses could always be estimated, regardless of their relative values.

It is of interest to mention some hydraulic fracturing results obtained in two oil fields in Ohio and Illinois<sup>19</sup>. Four and five

wells, respectively, were hydraulically fractured, the variation of pressure with time plotted, and the azimuth of the fractures recorded on oriented impression packers. All fractures were vertical, and within each field the results from well to well were remarkably consistent<sup>19</sup>, showing a strong dependency on the tectonic stresses prevailing there. The average values of pertinent data and results in the Ohio field were:  $D = 2650$  ft,  $P_o = 600$  psi,  $\sigma_t = 1000$  psi,  $P_c = 2975$  psi,  $P_s = 2225$  psi, fracture azimuth =  $69^\circ$  East of North. As the value of  $\alpha$  was unknown, Equations (7a) and (11a) could be used to approximate  $\sigma_{11}$  and  $\sigma_{22}$ :  $\sigma_{11} = -3500$  psi (acting at  $69^\circ$  East of North),  $\sigma_{22} = -1625$  psi.  $\sigma_{33}$  could be estimated from the assumed weight of the overlying rock:  $\sigma_{33} = -2050$  psi. In the Illinois field the average values were:  $D = 325$  ft,  $P_o = 0$ ,  $\sigma_t = 725$  psi,  $P_c = 650$  psi,  $P_s = 350$  psi, fracture azimuth =  $62^\circ$  East of North. Again using the same equations, the following values could be obtained:  $\sigma_{11} = -1125$  psi (acting at  $62^\circ$  East of North),  $\sigma_{22} = -350$  psi,  $\sigma_{33} = -325$  psi. The resulting principal tectonic stresses in both fields seem very reasonable with  $\sigma_{22} > \sigma_{33} > \sigma_{11}$  in Ohio and roughly  $\sigma_{22} \approx \sigma_{33} > \sigma_{11}$  in Illinois. Better approximations would have been obtained were the values of the porous-elastic parameters known.

The theoretical relationships developed, the encouraging laboratory experiments on fracture initiation, and field results like the ones just mentioned strongly indicate that hydraulic fracturing can be used to approximate the state of stress at great depth. However, more work is required in investigating the fracturing of anisotropic formations and the fracturing of rock

strata in which the principal in-situ stresses are not necessarily vertical and horizontal. The development of a reliable instrument that can detect the inclination and direction of a fracture away from the borehole, will give a considerable boost to the practical application of the method. Above all, more field tests are now necessary, possibly at shallow depths, so that they can be verified against well known methods of stress measurement. When this is done, hydraulic fracturing may soon cease to be a potential method and become a practical tool of stress determination.

## NOMENCLATURE

- $C_b$  = rock bulk compressibility  
 $C_r$  = rock matrix compressibility  
 $D$  = depth  
 $P$  = fluid pressure  
 $P_o$  = initial pore fluid pressure  
 $P_c$  = borehole critical (breakdown) pressure  
 $P_f$  = borehole pressure required to extend fracture  
 $P_s$  = borehole instantaneous shut-in pressure  
 $P_w$  = borehole pressure  
 $S_{ij}$  = stress tensor  
 $S_{11}, S_{22}, S_{33}$  = tectonic (in-situ) stresses  
 $\alpha$  = constant of porous-elastic material  
 $\theta$  = angle measured counterclockwise from the  
radius in the direction of  $S_{11}$   
 $\nu$  = Poisson's ratio  
 $\sigma_{ij}$  = effective-stress tensor  
 $\sigma_H$  = horizontal hydrostatic effective stress  
 $\sigma_x, \sigma_y, \sigma_z$  = mutually perpendicular loads applied to  
specimen  
 $\sigma_{rr}, \sigma_{\theta\theta}, \sigma_{zz}$  = principal effective stresses at the borehole  
wall  
 $\sigma_{rr}^{(1)}, \sigma_{\theta\theta}^{(1)}, \sigma_{zz}^{(1)}$  = principal effective stresses at the borehole  
resulting only from tectonic stresses

### NOMENCLATURE (Cont'd)

$\sigma_t$  = tensile strength of a hollow cylinder that is subjected to internal pressure and is vertically fractured

$\sigma_t^V$  = tensile strength of a hollow cylinder that is subjected to internal pressure and horizontal external loading and is horizontally fractured

### ACKNOWLEDGEMENTS

This research was conducted for the Missouri River Division, U. S. Army Corps of Engineers under Contract DA-25-006-ENG-14,764.

The authors wish to acknowledge the assistance of Dr. W. D. Lacabanne with experimental details.

They also wish to thank Halliburton Services for permitting the senior author to work on the manuscript, for typing the paper and preparing the figures.



## REFERENCES

1. Scheidegger, A. E.: "Stresses in Earth's Crust as Determined from Hydraulic Fracturing Data", Geologie und Bauwesen (1962), vol. 27, p. 45.
2. Hubbert, M. K. and Willis, D. G.: "Mechanics of Hydraulic Fracturing", Transactions, AIME (1957), vol. 210, p. 153.
3. Kehle, R. O.: "Determination of Tectonic Stresses through Analysis of Hydraulic Well Fracturing", Journal of Geophysical Research (Jan., 1964), vol. 69, p. 259.
4. Haimson, B.: "Hydraulic Fracturing in Porous and Nonporous Rock and Its Potential for Determining In-Situ Stresses at Great Depth", Ph. D. thesis, University of Minnesota, (July, 1968).
5. Biot, M. A.: "Thermoelasticity and Irreversible Thermodynamics", Journal of Applied Physics (1956), vol. 27, p. 240.
6. Anderson, E. M.: "The Dynamics of Faulting", Oliver and Boyd, Edinburgh and London, (1963).
7. Timoshenko, S., Goodier, J. N.: Theory of Elasticity, 2nd edition, McGraw Hill, New York (1951).
8. Nowacki, W.: Thermoelasticity, Pergamon Press (1962).
9. Biot, M. A. and Willis, D. G.: "The Elastic Coefficients of the Theory of Consolidation", Journal of Applied Mechanics (1957), p. 594.
10. Mann, R. L. and Fatt, I.: "Effect of Pore Fluids on the Elastic Properties of Sandstones", Geophysics (1960), vol. 25, p. 433.
11. Terzaghi, K.: Theoretical Soil Mechanics, J. Wiley, New York (1943).
12. Hubbert, M. K. and Rubey, W. W.: "Role of Fluid Pressure in Mechanics of Overthrust Faulting", Bulletin of Geophysical Society of America (1959), vol. 70, p. 115.
13. Barenblatt, G. I.: "The Mathematical Theory of Equilibrium Cracks in Brittle Fracture", Advances in Applied Mechanics (1962), vol. 7, p. 56.
14. Haimson, B. and Fairhurst, C.: "Initiation and Extension of Hydraulic Fractures in Rocks", Society of Petroleum Engineers Journal (1967), p. 310

#### REFERENCES (Cont'd)

15. Geertsma, T., de Klerk, F.: "A Rapid Method of Predicting Width and Extent of Hydraulically Induced Fractures", SPE 2458, to be published in Soc. Petr. Eng. J.
16. Zemanek, J.: "The Borehole Televier - A New Logging Concept for Fracture Location and Other Type of Borehole Inspection", Presented at Fall Meeting of SPE (AIME), Houston, (1968).
17. Anderson, T.O. and Stahl, E. J.: "A Study of Induced Fracturing Using an Instrumental Approach", J. Petr. Tech. (1967), p. 261.
18. Wawersik, W. - Personal Communication, University of Minnesota, (Dec. 1967).
19. Haimson, B. and Stahl, E. J.: "Hydraulic Fracturing and the Extraction of Minerals Through Wells", Proceeding of the Third Symposium on Salt, Cleveland, Ohio, (April 1969), to be published.

Table 1

Physical Properties of Rocks Tested

<u>Physical Properties</u>	<u>Tennessee Marble</u>	<u>Charcoal Granite</u>	<u>Mankato Dolomite</u>	<u>Berea Sandstone</u>	<u>Hydrostone, 30/100</u>	<u>Hydrostone, 32/100</u>	<u>Hydrostone, 35/100</u>
Young's Modulus (psi)	10.4 x 10 <sup>6</sup>	9.7 x 10 <sup>6</sup>	7.5 x 10 <sup>6</sup>	1.9 x 10 <sup>6</sup>	2.9 x 10 <sup>6</sup>	2.6 x 10 <sup>6</sup>	2.3 x 10 <sup>6</sup>
Poisson's ratio	0.28	0.32	0.25	0.20	0.22	0.22	0.215
Porosity (%)	2.3	2.2	9.5	18.8	24.9	25.9	27.0
Permeability (md)	-	-	0.7	190	8	11	17
$\alpha$				0.87	0.82	0.82	0.82
Compressive Strength (psi)	18,000	33,000	15,300	10,400	11,150	9,300	7,650
Tensile Strength- (psi) Brazilian Tests	1,800	1,700	1,900	750	1,720	1,600	1,430
$\sigma_t$ (psi)	3,000	2,400	3,500	1,750	1,650	1,200	950
$\sigma_v$ (psi)	3,050	3,200	5,600	3,450	1,800	1,700	2,050

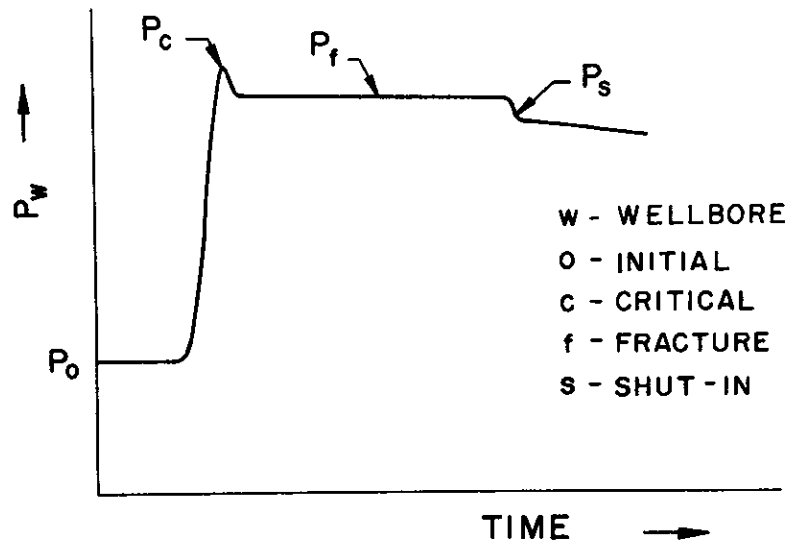


Fig. 1 - Borehole pressure-versus-time plot in a typical hydraulic fracturing operation.

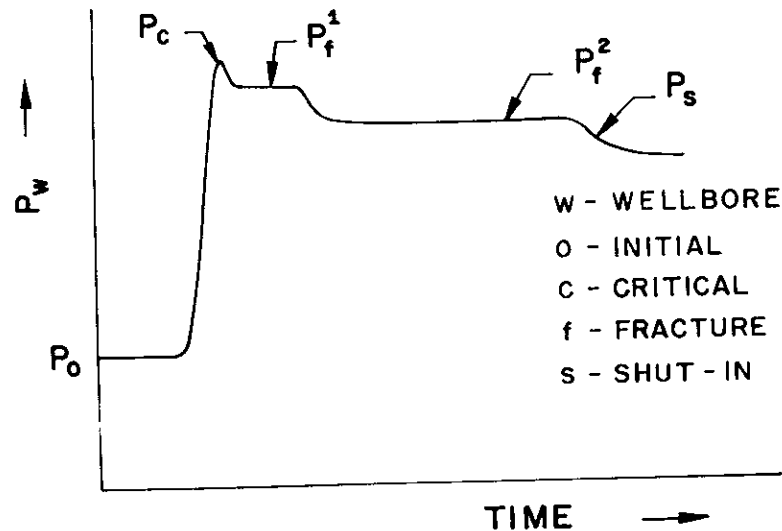


Fig. 2 - Hypothetical borehole pressure-versus-time plot when fracture initiates vertically, extends horizontally, and 'backs up' into the hole.

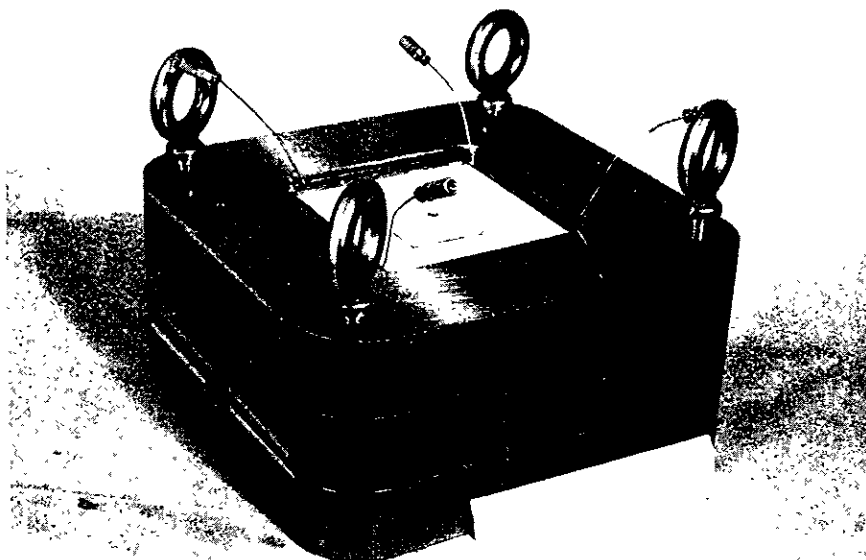


Fig. 3 - Steel frame with rock specimen and four flat-jacks.

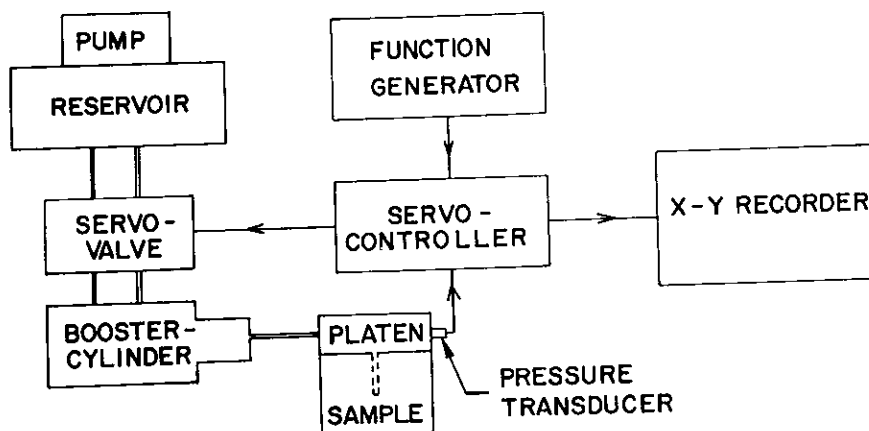


Fig. 4 - Block diagram of the automatic closed-loop borehole pressurization system.

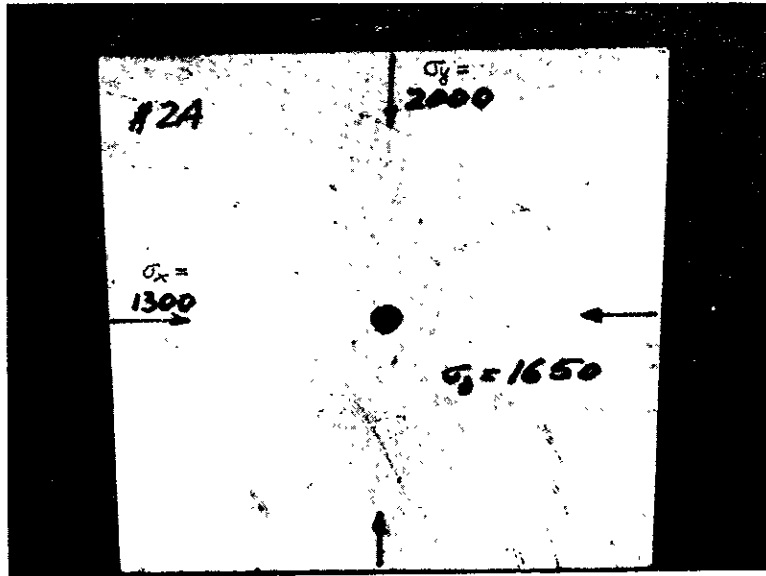


Fig. 5 - Vertical fracture in Tennessee Marble (horizontal section).

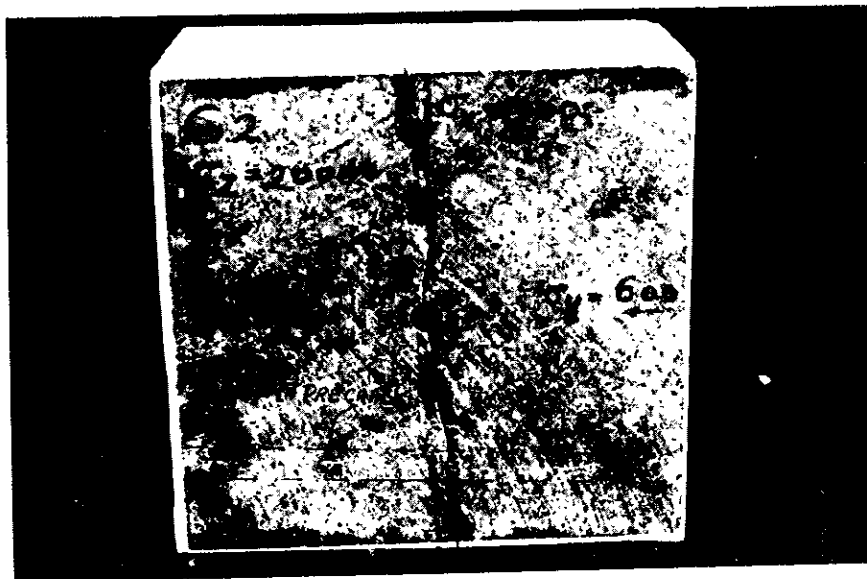


Fig. 6 - Vertical fracture in precracked Charcoal Granite (horizontal section).

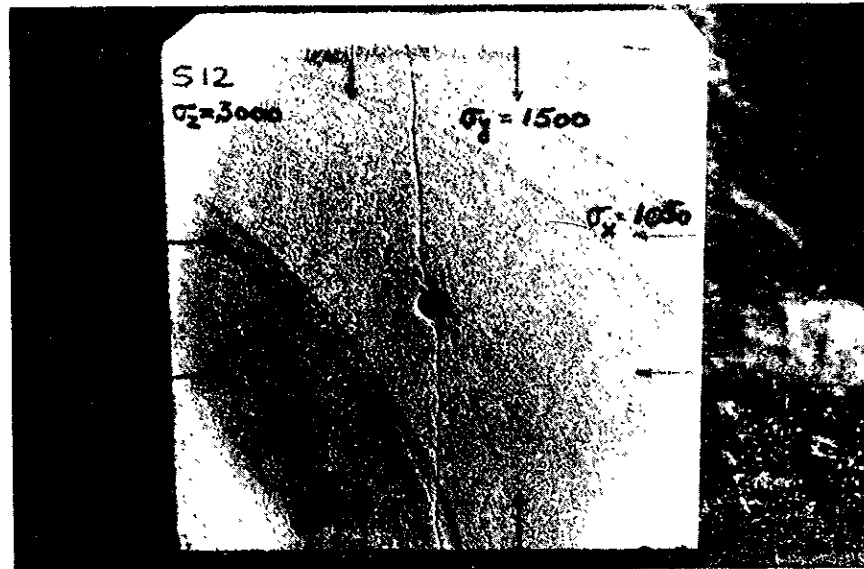


Fig. 7 - Vertical fracture in Berea Sandstone, showing the amount of fracturing fluid penetration (horizontal section).

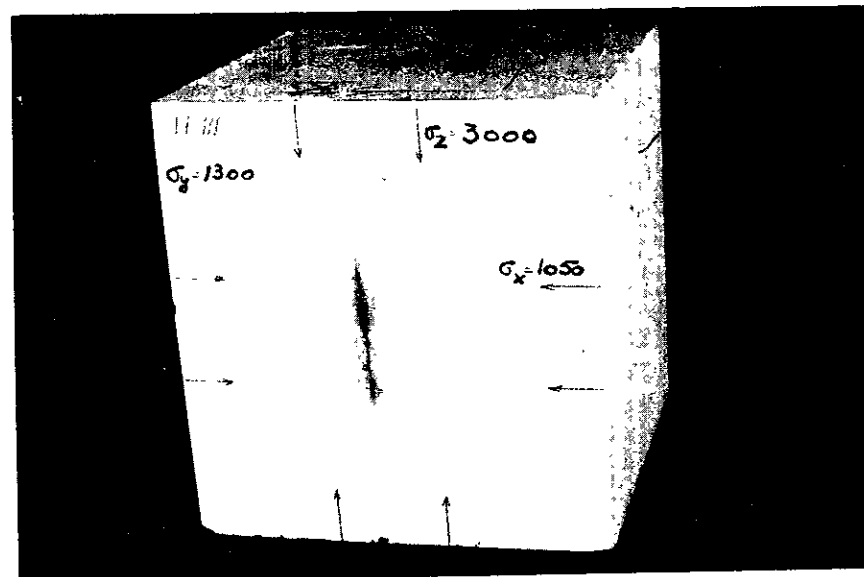


Fig. 8 - Vertical fracture in hydrostone.

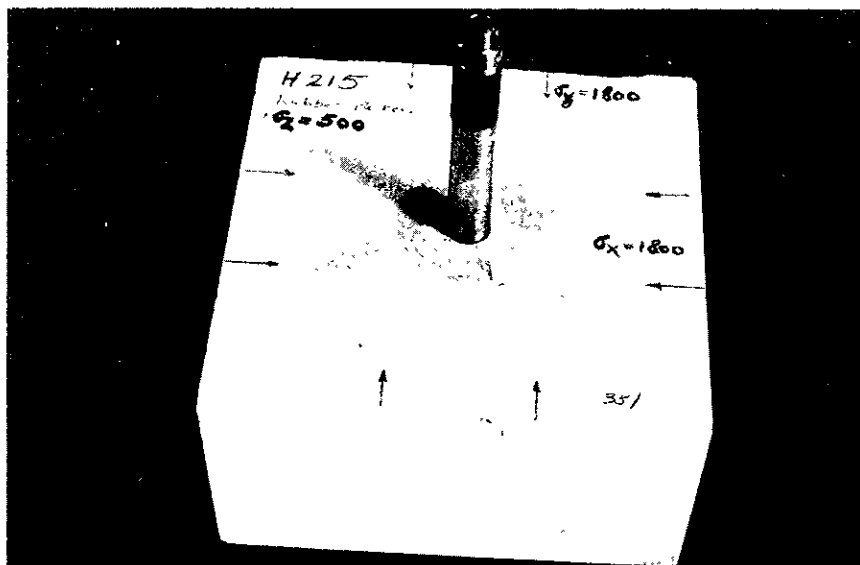


Fig. 9 - Vertical fracture in hydrostone, (horizontal section).

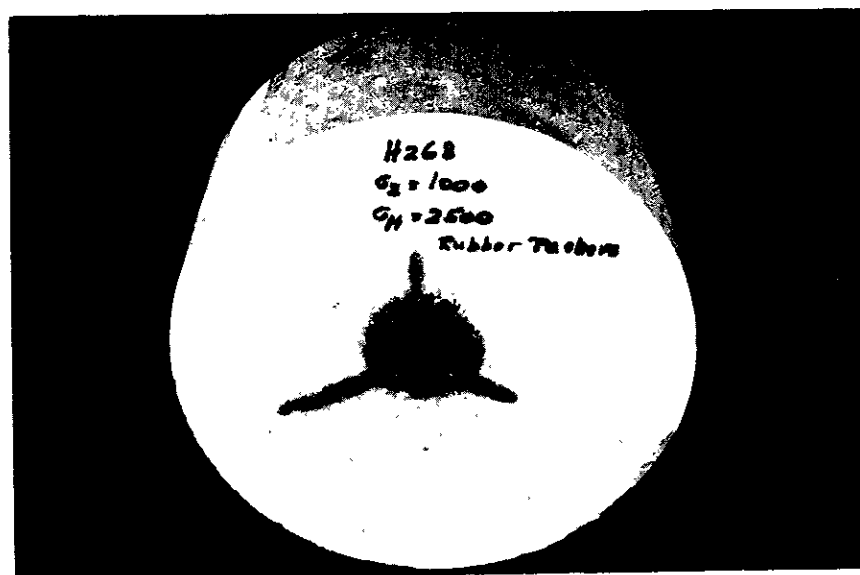


Fig. 10 - Three vertical fractures in a horizontal section of a hydrostone sample.



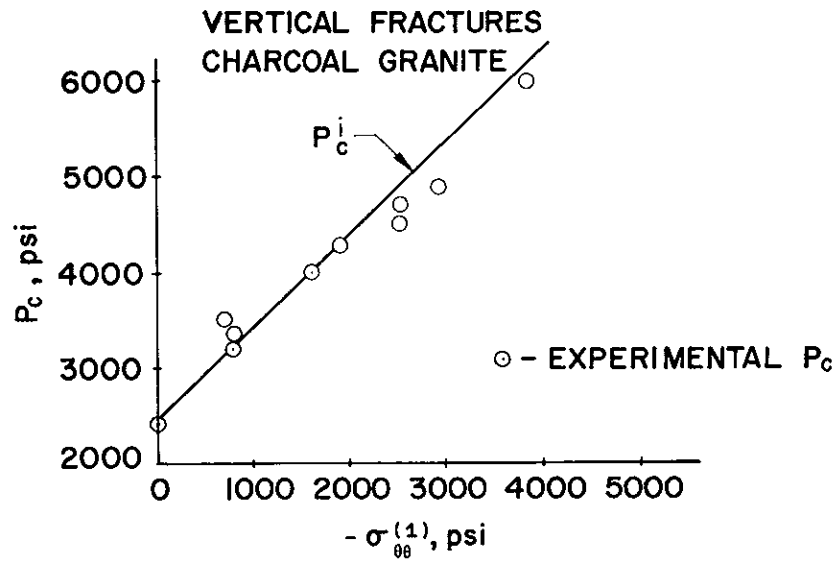


Fig. 11 - Breakdown (critical) pressure in Charcoal Granite versus  $\sigma_{\theta\theta}^{(1)} (= 3\sigma_{22} - \sigma_{11})$ .

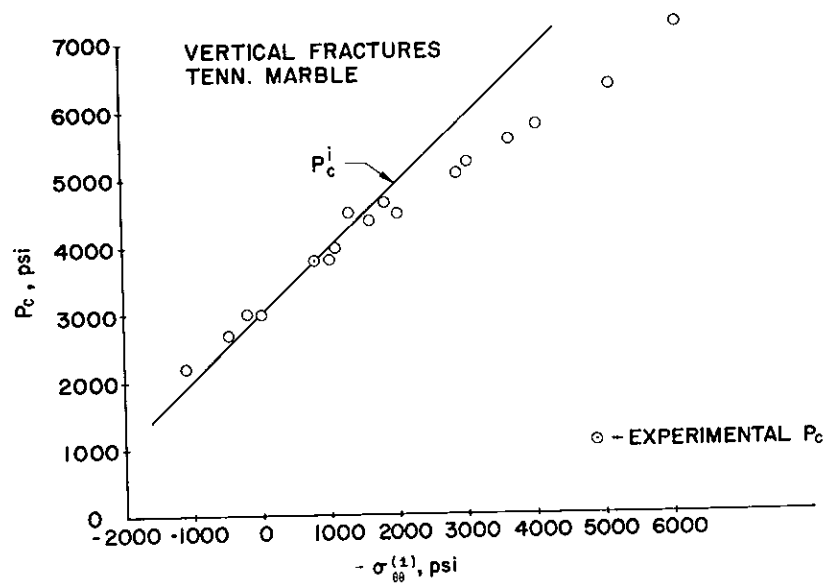


Fig. 12 - Breakdown (critical) pressure in Tennessee Marble versus  $\sigma_{\theta\theta}^{(1)} (= 3\sigma_{22} - \sigma_{11})$ .

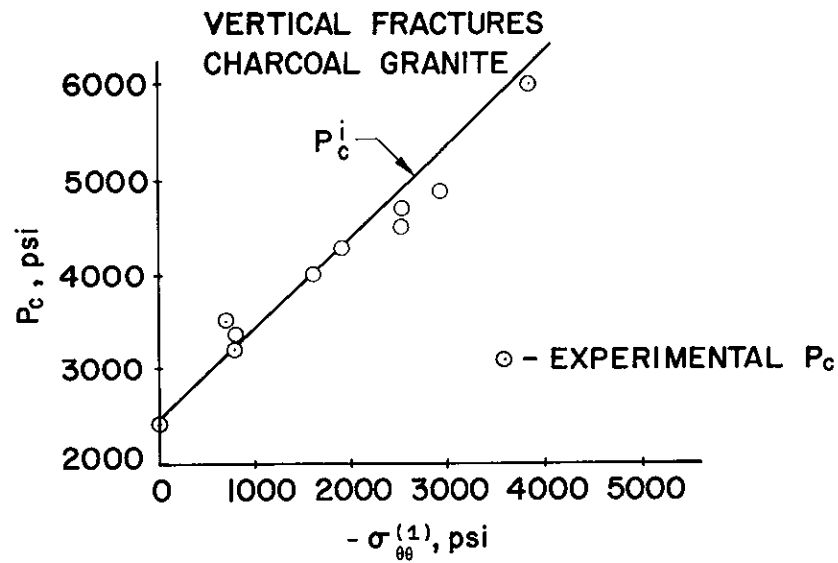


Fig. 11 - Breakdown (critical) pressure in Charcoal Granite versus  $\sigma_{\theta\theta}^{(1)} (= 3\sigma_{22} - \sigma_{11})$ .

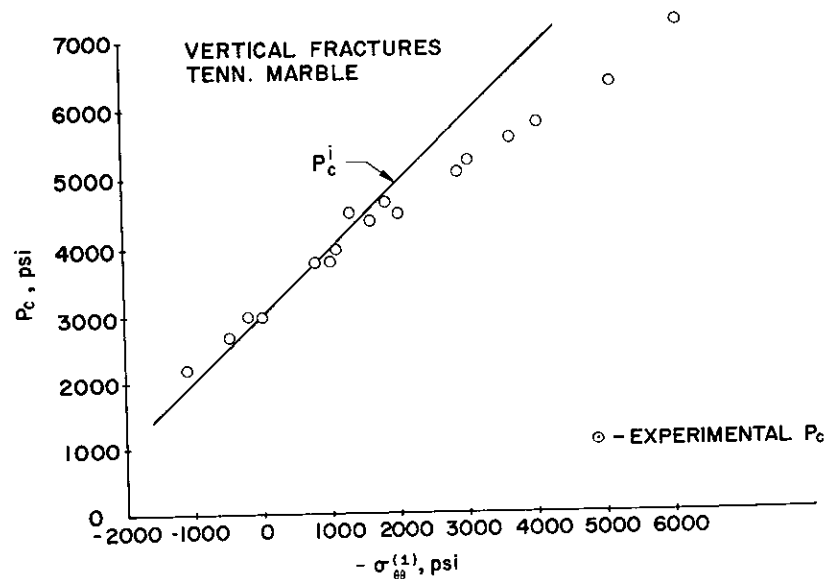


Fig. 12 - Breakdown (critical) pressure in Tennessee Marble versus  $\sigma_{\theta\theta}^{(1)} (= 3\sigma_{22} - \sigma_{11})$ .

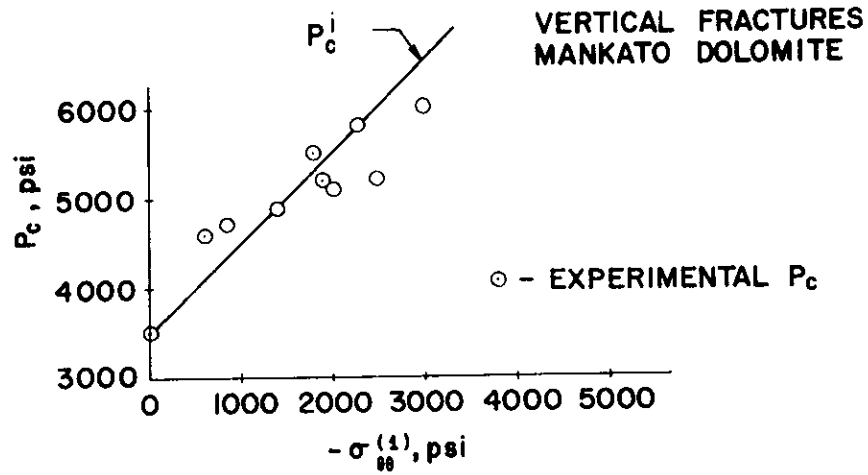


Fig. 13 - Breakdown (critical) pressure in Mankato Dolomite versus  $\sigma_{\theta\theta}^{(1)} (= 3\sigma_{22} - \sigma_{11})$ .

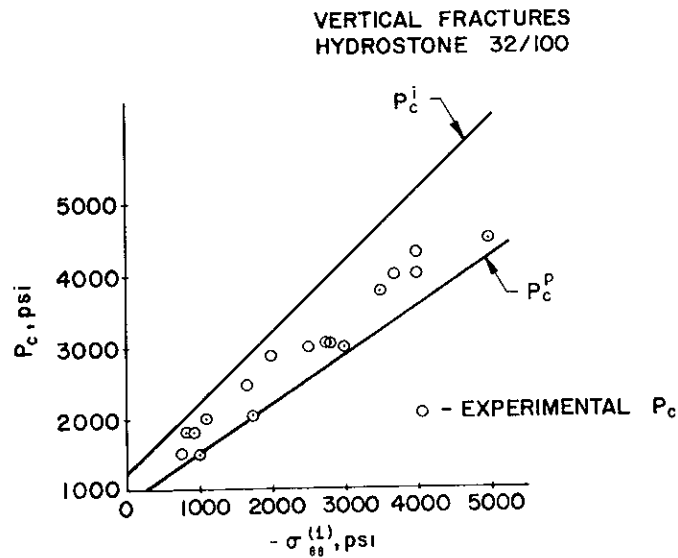


Fig. 14 - Breakdown (critical) pressure in hydrostone (32/100) versus  $\sigma_{\theta\theta}^{(1)} (= 3\sigma_{22} - \sigma_{11})$ .

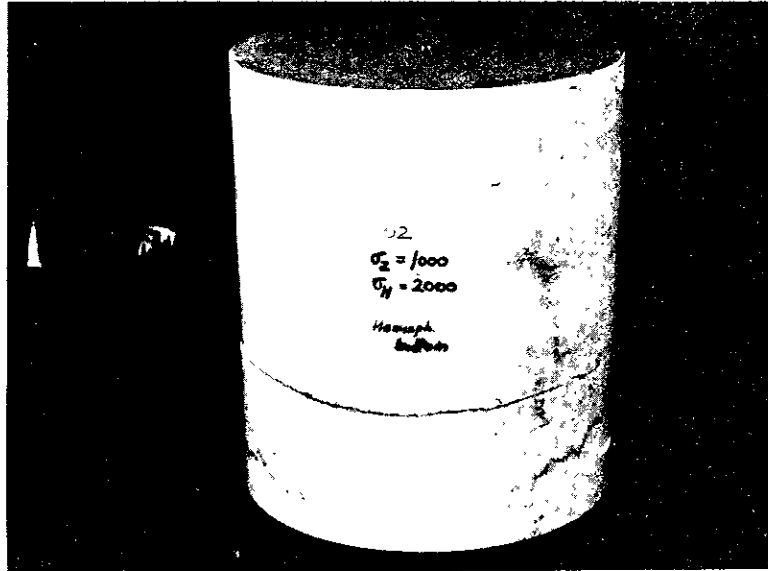


Fig. 15 - Horizontal fracture in Tennessee Marble.

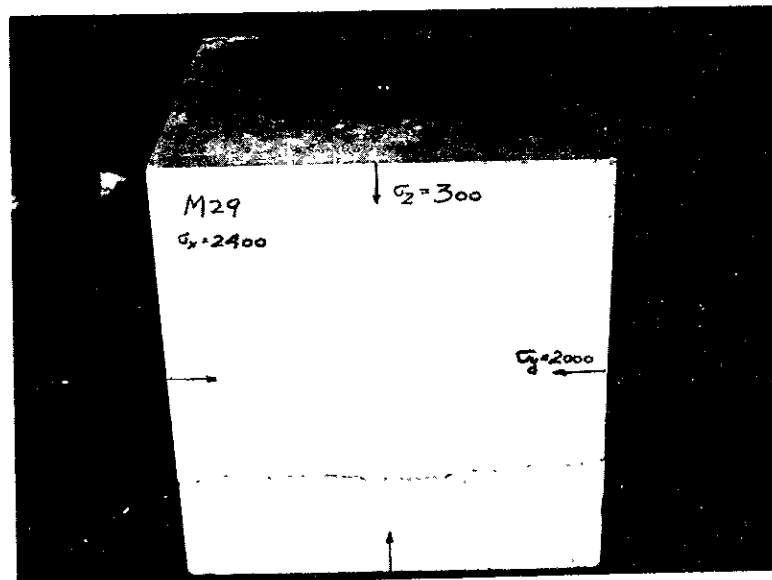


Fig. 16 - Horizontal fracture in Mankato Dolomite.

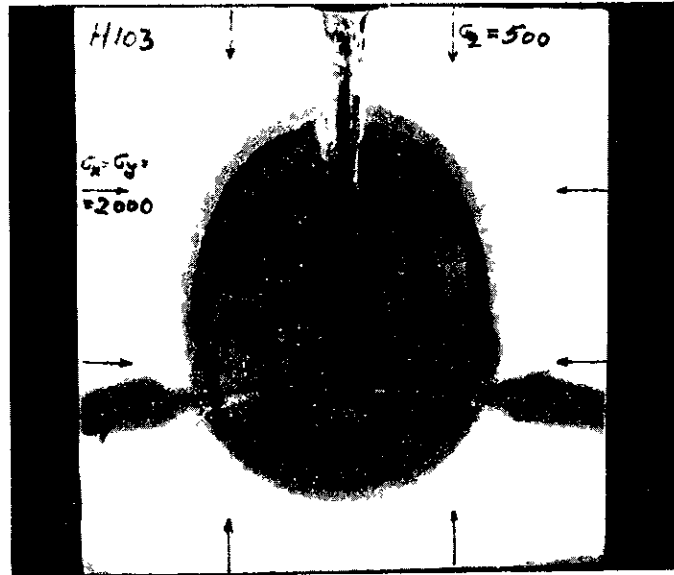


Fig. 17 - Horizontal fracture in hydrostone (vertical section).

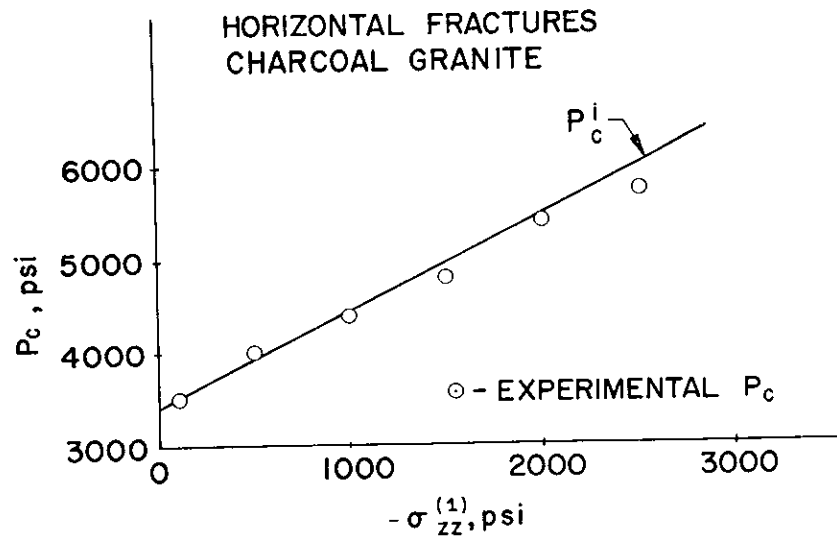


Fig. 18 - Breakdown (critical) pressure in Charcoal Granite versus vertical loading.

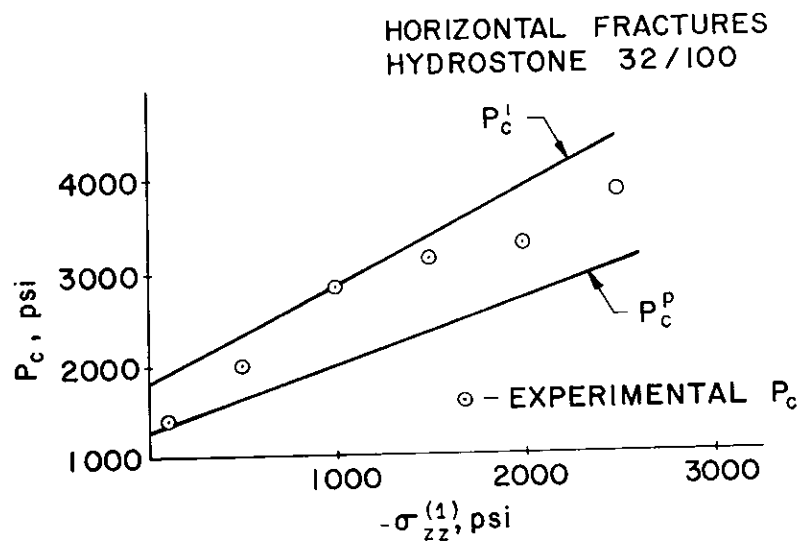


Fig. 19 - Breakdown (critical) pressure in hydrostone (32/100) versus vertical loading.

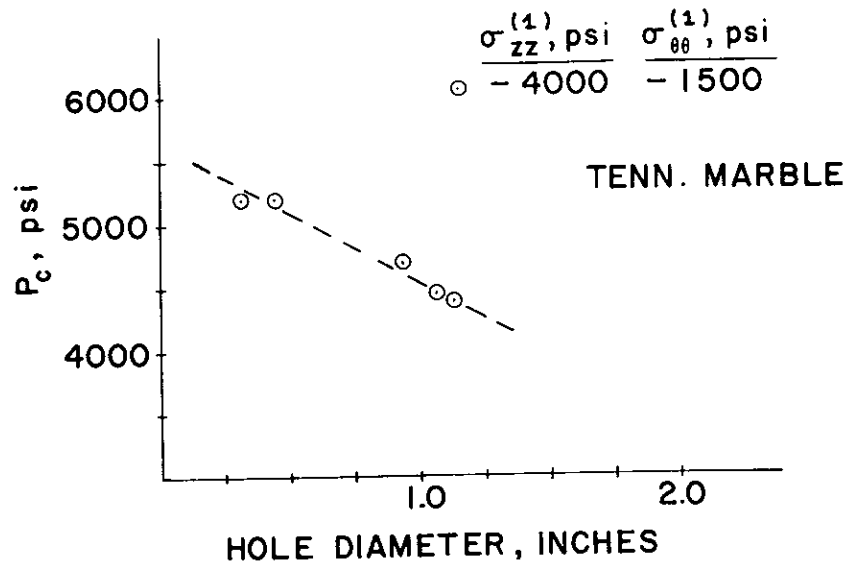


Fig. 20 - Effect of hole diameter on vertical fracturing breakdown pressure, in Tennessee Marble.

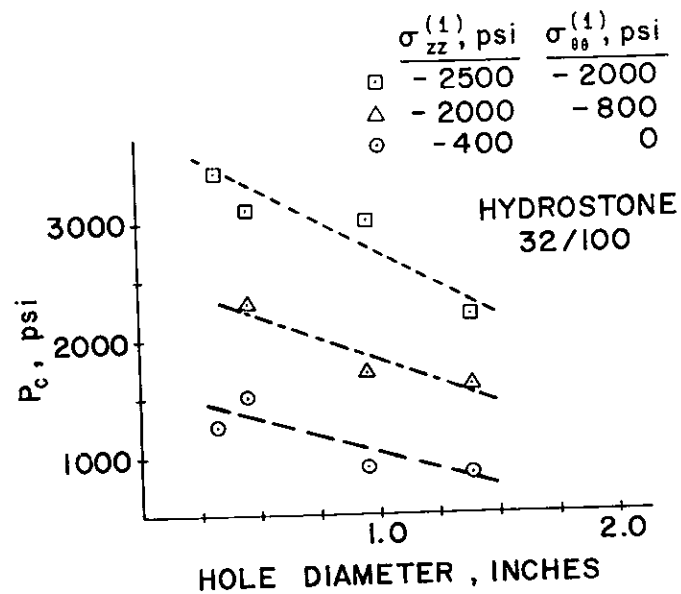


Fig. 21 - Effect of hole diameter on vertical fracturing breakdown pressure, in hydrostone 32/100.

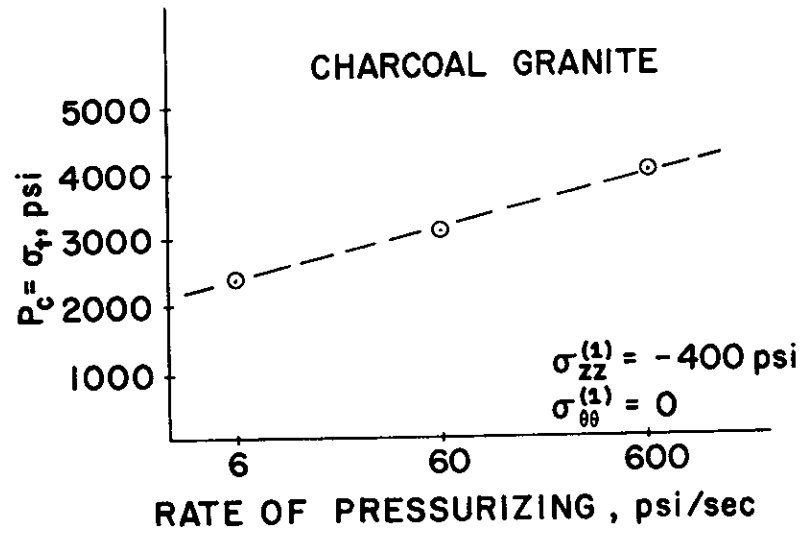


Fig. 22 - Rate of pressurizing effect on vertical fracturing breakdown pressure, in Charcoal Granite.

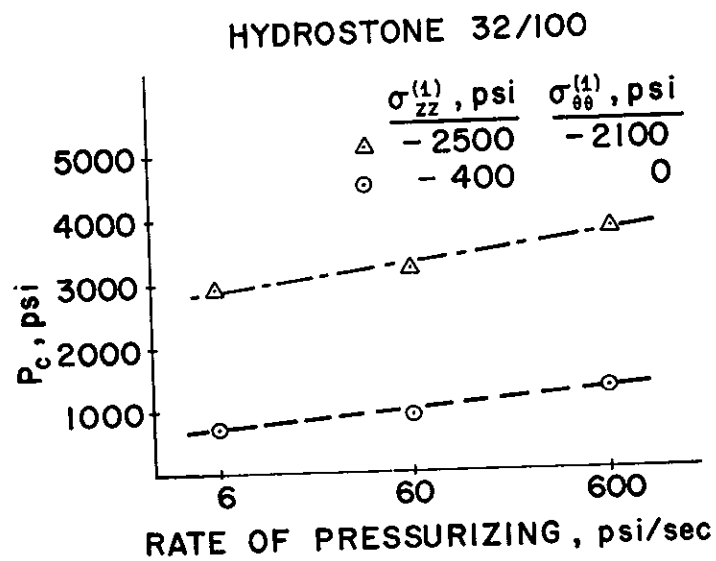


Fig. 23 - Rate of pressurizing effect on vertical fracturing breakdown pressure, in hydrostone 32/100.